Free Energy of Cavity Formation in Liquid Water and Hexane

Martine Prévost,* Isabel T. Oliveira, Jean-Pierre Kocher, and Shoshana J. Wodak

Unité de Conformation des Macromolécules Biologiques, Université Libre de Bruxelles, Avenue Franklin Roosevelt CP160/16, B-1050 Brussels, Belgium

Received: October 2, 1995; In Final Form: December 22, 1995[⊗]

The difference between the work of forming a cavity in water versus organic solvents is believed to play an important role in making apolar solutes less soluble in water than in these solvents, a property commonly referred to as the hydrophobic effect. In this study, two methods are applied, using molecular dynamics simulations, to compute the free energy of forming spherical cavities in the water and hexane liquids. One, based on the free energy perturbation approach, involves gradually growing into the liquid a soft cavity, by turning on a repulsive potential. The other computes the likelihood of finding a natural cavity in configurational data of neat liquids. In addition, the free energy of cavity formation in the two liquids is evaluated by the scale particle theory. Using all three approaches, we investigate how this free energy is influenced by the different descriptions of the cavity−solvent system: the perturbation method considers soft cavities whereas the statistical approach and scale-particle theory deal with hard sphere cavities. Also the scale-particle theory uses a simplified representation of the solvent while the computational procedures use an atomic description. The results of the perturbation approach show that it is more costly to accommodate a cavity of molecular size in water than in hexane, in agreement with previous evaluations, based on the statistical approach. In hexane, we obtain a rather similar cavity size dependence of the free energy computed with the two simulation methods. In principle, this should also be the case for water. We find, however, significantly higher free energy values in water with the statistical method than with the perturbation approach. This result is confirmed by an analysis of the structure of water around the cavities. Ways of bringing the two calculations to converge to the same result are discussed.

Introduction

Water and mixtures of water and organic molecules are commonly used as solvents for a large variety of organic reactions. Many investigations have shown that aqueous solvents relative to nonaqueous media affect in a remarkable way the rates and the thermodynamic parameters of these reactions. The hydrophobic effect, which refers to the property of apolar or slightly polar solutes to be less soluble in water than in apolar organic solvents, is a well-known property exhibited by water mixtures. Describing its physical origins is important not only for our understanding of solvation phenomena but also for identifying the factors responsible for the stabilization of the native structure of biological molecules such as proteins.[1,2]

Suprisingly, the molecular mechanism of hydrophobicity is still a matter of debate. To shed light on the phenomenon of hydrophobicity in terms of the structure and properties of liquid water as a solvent, the process of transferring a small nonpolar molecule from the gas phase into a liquid was broken up in two steps:[3] creating a cavity the size of the solute molecule and introducing the solute into the cavity by making it interact with the surrounding solvent molecules. In terms of the free energy costs, this accounts to

$$\Delta A_{sol} = \Delta A_c + \Delta A_{int} \qquad (1)$$

where ΔA_c is the work of cavity creation and ΔA_{int} that of the solute−solvent interaction. The first process takes into account the short-range repulsive part of the potential while the second process involves the attractive, long-range, soft part of the potential. An adequate treatment of both terms in (1) is necessary to fully describe the thermodynamics of the process. Solvent reorganization contributes to both terms.[4] The work of cavity creation is entirely due to solvent reorganization around the cavity. Lee showed that, at room temperature, solvent reorganization caused by turning on the attractive potential is negligible both in water and organic liquids.[4] Moreover, the interaction of apolar solutes with the hydrocarbon solvents and with liquid water was estimated to be similar.[4] Based on these two considerations, ΔA_{int} in (1) is similar for the two types of solvents at room temperature. This therefore suggests that the difference between the free energy of cavity formation in the organic and water solvents should be responsible for hydrophobicity.

ΔA_c is not a directly measurable experimental quantity; estimates of ΔA_c can be obtained either from scale particle theory (SP) or from simulation methods. SP theory[5] uses a simplified description of the solute and makes use of experimental bulk parameters to model the solvent. It assigns excluded volumes to the solvent molecules, assumes that the properties of the solvent are inherent in the density of the pure liquid, and considers the volume accessible to a hard-sphere solute. Directional interactions, such as hydrogen bonds, are hence not accounted for. Applications of the scale particle model[6−8] to studies of inert gases in molecular liquids have shown that the work of cavity formation is larger in water than in most of the common organic solvents. This has led to the suggestion that the origin of this difference is not due to the structure of liquid water[4] but is chiefly due to the small size of the water molecule relative to that in the organic molecules.[4,9]

To test this physical picture of the mechanism of hydrophobicity, Pohorille and Pratt[10,11] undertook a study of the free energy of cavity formation in water and in various organic

* To whom correspondence should be addressed. Phone: 32 2 648 5200. Fax: 32 2 648 8954. E-mail: martine@ucmb.ulb.ac.be.

[⊗] Abstract published in *Advance ACS Abstracts,* February 1, 1996.

0022-3654/96/20100-2738$12.00/0

solvents. This quantity was evaluated from thermally equilibrated configurations of the liquid obtained from computer simulations, by computing the likelihood of encountering spherical cavities of a given size at a given point in the liquid,[12] a method referred to here as the test-particle method (TP). Their results showed that for large cavities (>1.1 Å radius), the free energy cost for cavity formation is larger in water than in the organic solvents and they concluded that the free volume is distributed in smaller packets in water than in those solvents. Madan and Lee[13] used the same approach to compute the free energy of cavity formation in liquid water and in a Lennard-Jones "reference liquid" for which the most probable distance between two molecules is that found in water. They found that the free energy of cavity formation is approximately equal in both liquids suggesting that changes in the hydrogen-bonding structure and the orientational degrees of freedom of water are not essential in producing the large free energy of cavity formation in water. A similar comparison made with a Lennard-Jones liquid defined so as to reproduce the most probable intermolecular distance as well as the pressure of liquid water led to opposite conclusions.[11]

Another method for computing the free energy of cavity formation in liquids from computer simulations is based on the free energy perturbation approach.[14] This procedure, termed here the repulsive particle (RP) method, deals with soft cavities which are gradually grown into the liquid by turning on an inverse 12th power repulsive potential describing the interaction between the cavity and the solvent molecules. It has, to our knowledge, been applied only to compute the free energy of cavity formation in water, but not in organic solvents.

In light of all the above considerations, there clearly is a need for a systematic investigation of the process of cavity formation as a function of different cavity shapes and sizes, and of how different liquids respond to this process.

In this study, the two simulation methods, RP and TP, are applied to compute the free energy of forming spherical cavities in water liquid and the organic liquid, hexane. The results obtained from both procedures are compared and confronted with evaluations using SP theory. In particular, we investigate the differences in the work of cavity formation computed with RP in the two liquids as a function of the cavity size. Furthermore, given that the RP procedure considers soft cavities whereas TP and SP theory consider hard spheres and that the system is described in atomic detail in TP and RP but is simplified in SP theory, we also analyze to what extent these different descriptions influence the results. In the case of RP and TP, we also compare the structure of the liquid surrounding the cavities and discuss the observed differences.

Methods

a. The Test-Particle Method (TP). This method relies on a statistical analysis of configurations generated in simulations of the pure liquid system. The Helmholtz free energy ΔA_c of cavity formation is calculated using the following formula[12]

$$\Delta A_c = -RT \ln p(R_c) \tag{2}$$

where $p(R_c)$ is the probability of finding a cavity of radius R_c at a given point in the simulated liquid; R is the gas constant and T the temperature. This probability is computed as[12]

$$p(R_c) = \langle V_{R_c} \rangle / V \tag{3}$$

where V_{R_c} is the volume accessible to a test particle consisting of a hard sphere of radius R_c and V is the total volume of the system. The brackets in (3) indicate the ensemble average over configurations of the solvent unaffected by the test particle. In practice, the volume ratio V_{R_c}/V is computed by defining a cubic lattice with fixed spacing (here, 0.5 Å) and counting the number of lattice nodes that fall within a cavity of a given size and dividing this number by the total number of nodes in the entire system. This computation is repeated for each configuration in the trajectory, and the results are summed over all the nodes and all the configurations.[10]

b. The Repulsive Particle Method (RP). In the RP method,[14] a soft cavity is gradually grown at a fixed location in the simulated liquid by means of a short-range repulsive potential:

$$V_{cav} = \lambda V_{rp} = \lambda \sum_i 4\epsilon_i(\sigma_i/r_i)^{12} = \lambda \sum_i (B_i/r_i)^{12} \tag{4}$$

V_{rp} is the repulsive part of the Lennard-Jones potential, with the parameters σ_i and ϵ_i characteristic of the atom i with which the repulsive particle embodying the soft cavity interacts. B_i is defined as $(4\epsilon_i)^{1/12}\sigma_i$; r_i is the distance between the repulsive particle and the atom i. λ is a parameter that scales the strength of the repulsion and hence the size of the cavity. Increasing the values of λ in small steps allows to gently grow a cavity into the liquid.

To evaluate the free energy cost of cavity formation ΔA_c, the thermodynamic integration method (TI)[15] is used:

$$\Delta A_c = \int_0^1 \left\langle \frac{\partial V_{cav}(\lambda)}{\partial \lambda} \right\rangle_\lambda d\lambda \tag{5}$$

In this method, the ensemble average of the derivative in (5) is integrated over λ values ranging from 0 (a liquid without a cavity) to 1 (a fully grown cavity). The ensemble averages are obtained from molecular dynamics simulations, performed with discrete λ values.

c. Scale-Particle Theory (SP). The application of the SP theory to solutions[7] is used primarily as a means of determining the reversible work required to introduce a hard-sphere molecule into a fluid whose molecules behave as hard cores but whose density at a given temperature is determined by the real intermolecular potentials. The reversible work to create a mole of hard-sphere cavities with a radius R_c, the latter being defined so that any part of the solvent molecules are excluded from a spherical region of radius R_c, is given by[5]

$$\Delta A_c = -RT \ln\left[1 - \frac{4\pi}{3}((R_1/2) + R_c)^3\rho\right] \qquad R_c \le R_1/2 \tag{6}$$

and

$$\Delta A_c = K_0 + K_1 R_c + K_2 R_c^2 \qquad R_c \ge R_1/2 \tag{7}$$

where

$$K_0 = RT[-\ln(1-y)] \tag{8}$$

$$K_1 = \frac{RT}{R_1}\left[\frac{6y}{(1-y)}\right]$$

$$K_2 = \frac{RT}{R_1^2}\left[\frac{12y}{(1-y)} + 18\left(\frac{y}{1-y}\right)^2\right]$$

R_1 is the hard-sphere diameter of the solvent, $y = \pi(R_1)^3\rho/6$ is the volume fraction of the solvent spheres and ρ is the solvent number density. The terms involving the pressure have been neglected since they are insignificant for molecular-sized cavities at low pressure. The values of the parameters used to compute the quantities in (6)−(8) are given in Table 1.

TABLE 1: Values of the Parameters Used in SP Theory Calculations[a]

	R_1(Å)	ρ
hexane	6.0	0.0046
water	3.17/2.8	0.033

[a] R_1 is the solvent diameter and ρ is the solvent number density.

Simulation Conditions. To generate the configuration ensembles for hexane and water, MD simulations were performed using the CHARMM package.[16] The hexane molecule was modeled[17] using the united atom representation for the CH_n groups where each group is represented by a unique interaction center. In this model, the CH_2 and CH_3 groups have identical σ values but their ϵ values differ (Table 2). Liquid water was simulated using the three-point charge SPC model.[18] In this model, a single Lennard-Jones interaction center is positioned at the oxygen nucleus (Table 2).

TABLE 2: Values of the Energy Parameters (See Eq 4) Assigned to the Interaction Sites of the CH_n Groups in Hexane and of the Oxygens in Water

	σ(Å)	ϵ (kcal/mol)
CH_2 (hexane)	3.906	0.118
CH_3 (hexane)	3.906	0.175
oxygen (water)	3.1656	0.1554

For both the TP and RP calculations, the hexane simulations were performed on 125 molecules. The water simulations were done on a box of 216 and of 343 molecules for RP and TP, respectively. Periodic boundary conditions were applied and long-range interactions were smoothly truncated at 14 Å for hexane and 8.5 Å for water.

All the simulations were performed in the microcanonical ensemble at the solvent density corresponding to the normal experimental value for a temperature of 300 K.

Trajectories of 1 ns of both hexane and water were generated for the TP calculations.

For the RP calculations, 27 successive simulations were performed for λ values ranging from 10^{-6} to 1. For each λ value, the system was first subjected to an equilibration period of 10 ps, after which a 50 ps production trajectory was generated for analysis. The total length of the trajectory used to fully grow the cavity was 1.62 ns.

Evaluating the Cavity Radius. RP and TP represent two different procedures for computing the free energy cost of cavity formation in liquids. The only formal difference between them is that RP considers the cavity as a soft particle while TP defines the cavity as a hard-core spherical particle, as does SP theory. To be able to compare the ΔA_c values obtained by the three approaches, it is necessary to derive, in RP, the corresponding hard-sphere radius of a cavity whose intermolecular potential varies as $1/r^{12}$. This is done using the method derived by AWC.[19−21] In applying this method here to compute the hard sphere cavity radius in hexane, we use the energy parameters of the CH_2 group. This choice can be justified by the fact that the CH_2 and CH_3 parameters differ only slightly (Table 2) and that, moreover, CH_2 is the main aliphatic group of this molecule.

In defining the cavity size, two related, but different measures can be used. One is the center-to-center distance R, defined so that the centers of the solvent molecules are excluded from a spherical region of radius R. The other is the cavity radius R_c, defined as the distance from which any part of the solvent molecules is excluded. When the solvent molecules are hard spheres of diameter R_1, the two definitions of cavity size are related by $R = R_1/2 + R_c$. When comparing different solvents, R_c has to be used. Thus, throughout this study, the free energy results are reported as a function of the cavity radius R_c. R_c is dependent on the diameter of the solvent molecules, to which different authors assign different values.

In the hexane SP calculations, we take a value of 6 Å for the hard sphere diameter representing the entire molecule, in accord with estimates of effective radii for *n*-hexane.[22] To evaluate R_c, in the hexane RP and TP calculations, we assign a diameter of 3.9 Å to the CH_2 groups.

In water, the problem of assigning a diameter to the solvent molecules is not trivial. There are two options: use the effective hard core diameter of the solvent molecules given by the Lennard-Jones σ parameter or the most probable distance of approach between two water molecules derived from the position of the first peak in the radial distribution function. Considering the cavity as a substitute for a nonpolar solute that does not hydrogen bond to water, we use the σ value to derive the cavity radius as previously proposed.[13]

For both liquids, in TP and RP, the cavity radius R_c is computed subtracting from the cavity−solvent group center-to-center distance half the σ value of the corresponding solvent group. Note that in SP theory the solvent diameter is a parameter in the equations. To compute the free energies with this theory, we use in turn the effective hard core diameter and the most probable distance of approach.

Results and Discussion

Work of Cavity Formation in Hexane and Water Computed with the RP Procedure. To compare the behavior of the two liquids and interpret the results in terms of the hydrophobic effect, the work of cavity formation ΔA_c was monitored as a function of the cavity radius R_c. To allow direct comparisons with the results obtained by TP and SP (see below), this cavity radius was computed from the soft repulsive potential at each λ, using the AWC theory,[19,20] and hence represents the hard-sphere cavity radius corresponding to this potential.

At λ values smaller than 10^{-4}, the cavity radius becomes negative, an indication that the cavity center samples the interior of the surrounding water molecules. The work of cavity formation computed at $R_c = 0$ can thus be related to the packing density of the liquid. To adequately estimate the packing density contribution to ΔA_c, simulations at very small λ values should be performed. In practice, it is difficult to correctly evaluate the ensemble average of the integrand of (5) since the statistical error increases as the λ value decreases. Another reason is that the extrapolation downward from simulations at small λ values is not reliable. Moreover, at very small λ, corresponding to very small cavity radii, the potential of eq 4 may become numerically unstable.

Following these considerations, the λ-simulations corresponding to negative cavity radii were not considered in the analysis, and the ensemble average in (5) was integrated starting from λ values of 2×10^{-4} and 10^{-4} for hexane and water, respectively. To compute the packing density contribution to ΔA_c (the ΔA_c value at $R_c = 0$) we took that obtained with eq 6 at $R_c = 0$. This contribution was added to the ΔA_c values computed from the simulations.

Figure 1 displays the ΔA_c values computed for hexane and for water as a function of the hard-sphere cavity radius R_c. We see that for radii up to 1.4 Å the curves of both liquids are rather similar, whereas for $R_c > 1.4$ Å, the ΔA_c values are higher in water than in hexane, with the water curve displaying a higher curvature than that of hexane.

The accuracy of the considered ΔA_c values is influenced by essentially two factors: the convergence of the simulations and the statistical imprecision. To ensure convergence of the calculations,[23] the configuration space was carefully sampled, especially in the interval of $\lambda < 0.1$, where the free energy rises

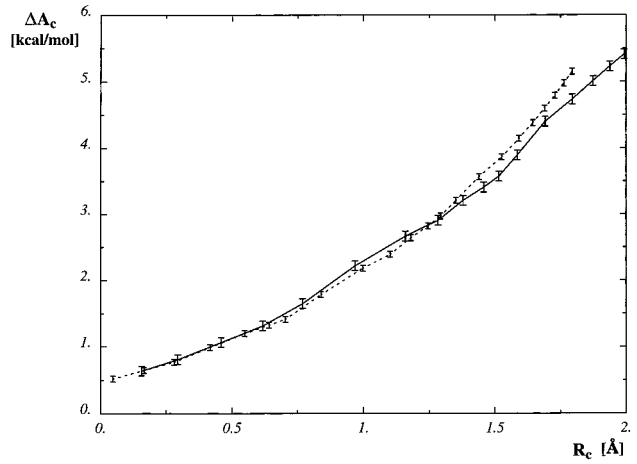

Figure 1. Work of cavity formation ΔA_c computed with RP method as a function of the radius of the cavity R_c in hexane (—) and in water (- - -). For hexane, the curve corresponds to an evaluation of the cavity radius using the energy parameters of the CH_2 group. The statistical error is represented by vertical bars.

abruptly. The main source of the statistical imprecision in the calculations is the finite length of the trajectories, from which ensemble averages are computed. In the RP procedure, this imprecision is caused by the fluctuations of $\langle V_{rp} \rangle$. To evaluate it, the statistical errors were computed, taking into account the time interval for which correlations persist between V_{rp} values of successive configurations.[24] We see that these errors, displayed in Figure 1, reach at most 0.1 kcal/mol.

The higher curvature of the water curve relative to that of hexane (Figure 1) suggests that the free energy of cavity formation should become significantly larger in water for large enough cavity sizes, even though for radii less than 1.4 Å the work of cavity formation is similar in both liquids. To confirm this observation, the ΔA_c values were fitted by a polynomial of the form $A_0 + A_1R_c + A_2R_c^2$. The choice of this polynomial is suggested by the quadratic behavior of the work of cavity formation in SP theory as a function of the cavity radius (see eq 7). The obtained fits are excellent for both curves, with values for the coefficient in R_c^2 of 0.75 for the hexane curve and 1.2 for the water curve. This clearly indicates that the work of cavity formation in water should exceed that in hexane for cavities of large enough radii.

Pohorille and Pratt[10] observed a similar result for large cavity radii using the TP method with simulations of the TIP4P water model. However, for smaller radii they obtained higher ΔA_c values in hexane than in water, which they suggested to result from the lower packing density of water. The ΔA_c values clearly depend on the diameter assigned to the particles in the system. As discussed in Methods, the choice is unambiguous for hexane, but not for water, where taking into account electrostatic interactions leads to a smaller diameter (2.8 Å) than that given by the σ parameter (3.17 Å). We considered the larger diameter in computing R_c, whereas Pohorille and Pratt's results were obtained with the smaller value. Using the smaller diameter here brings the behavior of our free energy values into agreement with their results (data not shown).

Comparison of the RP Results with Those of the TP and SP Calculations. In this section, we compare the cavity size dependence of ΔA_c in hexane and water, computed with the RP and TP methods. These results are furthermore compared to estimates made using SP. Figure 2 displays the ΔA_c values plotted as a function of the hard-sphere radius R_c.

Some trends common to both solvents can be observed when one uses the same water diameter (here 3.17 Å) in RP, TP, and SP. In comparing all three calculations, we see that the behavior

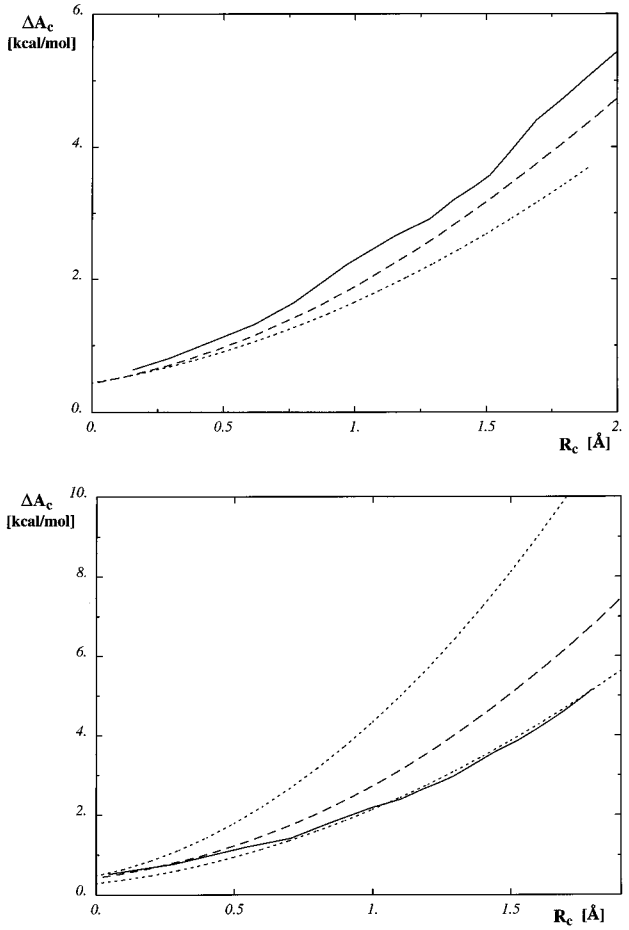

Figure 2. Comparison of the work of cavity formation ΔA_c computed with the two simulation methods RP (—) and TP (— — —) and with SP theory (- - -) as a function of the radius of the cavity R_c in hexane (a, top) and in water (b, bottom). In water, the upper and lower SP curves were computed with the σ (3.17 Å) and the most probable distance (2.8 Å), respectively.

at large cavities ($\geq$1 Å) diverges. At $R_c = 0$, on the other hand, the curves computed with TP and SP theory converge, indicating that the liquid packing densities in our TP calculations are similar to those computed using SP theory. Direct evaluation of the packing density cannot be made from the RP calculations, since the free energies for very small cavity sizes were not reliable enough to be considered in the analysis.

1. The Behavior in Hexane. For hexane (Figure 2a), SP yields lower ΔA_c values, than the two computational methods for all radii considered. This result is not unexpected. Indeed the TP and RP methods both use an atomic representation, even if only the united atom model (where aliphatic hydrogens are not explicitly represented), whereas SP theory uses a single hard sphere to describe the large nonspherical hexane molecules. We have seen, on the other hand, that liquid packing densities computed with TP and SP theory are similar ($\sim$0.5), suggesting that the diameter of 6 Å assigned to the hexane molecule in the SP theory equations leaves an identical free volume fraction as that present in the TP simulations. Thus, though SP theory predicts correctly the work of forming sufficiently small cavities, it fails to do so for larger cavities, where the detailed molecular structure comes into play, in agreement with earlier conclusions.[7]

The ΔA_c values computed with RP are higher, over the entire range of cavity radii, than those obtained with TP and SP (Figure 2a). This could be due to the fact that in RP, the cavity radius is computed only with the CH_2 energy parameters, which leads to underestimating its value, and hence to an upward shift of the RP free energy curve. With a cavity radius computed using the CH_3 energy parameters, significant differences between the

RP and TP results are no longer observed (data not shown). Another reason could be that in TP, hexane was simulated at a slightly higher temperature (305 K) than the various λ-simulations (298−300 K) in RP. Since one can expect a lower cost in cavity formation at higher temperatures,[4] this could to some degree explain the difference between TP and RP results.

2. The Behavior in Water. Figure 2b displays the ΔA_c curves obtained for water using RP, TP, and SP theory. For SP theory, the ΔA_c estimates were made with R_c values computed using the water diameters of 3.17 Å (SP3.17) and 2.8 Å (SP2.8), respectively. For RP and TP, we used only the larger water diameter in the evaluation of R_c, as stated in Methods.

We find that the SP3.17 curve rises faster than the TP curve. This can be rationalized by the fact that two different water sizes come into play in the TP results: the smaller diameter of 2.8 Å, representing the most probable water−water distance in the configuration ensemble used to compute the ΔA_c values, and the larger diameter (3.17Å), used to calculate the cavity radius R_c. In SP3.17, on the other hand, only the larger diameter is used to compute the free energy values with eqs 6 and 7.

The TP ΔA_c values and those of SP3.17 converge at zero cavity radius. This indicates that the two methods yield very similar packing densities for water (∼0.5). Not unexpectedly, the SP2.8 values are lower than the TP values. Indeed, using the smaller water diameter increases the empty space between the water molecules, making it easier to insert a cavity between them. On the other hand, when we use the same smaller water diameter to replot the TP free energies (data not shown), we still find higher free energy values with this method than with SP2.8. This latter result was obtained earlier by Pohorille and Pratt[10] who proposed that this was due to the hard-sphere solvent being able to find more ways to configure the free volume into packets of sufficiently large size.

Significant differences are displayed by the ΔA_c values computed with the RP and TP methods. In particular, for cavity sizes >1 Å the cost of cavity formation is larger for TP than RP. This indicates that it is significantly easier to insert a cavity into the solvent in the RP simulations, implying that the packing of water molecules around the cavity is lower in these simulations. To understand what causes this discrepancy, additional simulations are needed to monitor the effects of limiting the size of the system and imposing a constant volume. The former aspect could be dealt with by performing the RP simulations with the same box size as in TP. Simulations at constant pressure should help in dealing with compression problem resulting from the creation of cavities of substantial size in the liquid when molecular dynamics simulations are performed at constant volume. It is furthermore possible that both the TP and RP calculations encounter convergence problems despite the use of a rather long trajectory (1.6 ns in RP and 1 ns in TP). Longer simulations may be needed for the system to reach equilibrium when one deals with larger cavities. Also, the possibility that the observed differences are caused by the soft versus hard cavity radii used in RP and TP, respectively, cannot be ruled out, although the cavity radii in RP were computed in such a way that thermodynamic and structural properties are related to those of a corresponding hard-sphere system.

Postma et al. found a rather good agreement between their water ΔA_c values derived from RP and those computed with SP theory. However, this could be due to the use, by these authors in their SP calculations, of a slightly but significantly larger water diameter (2.875 Å), and furthermore, to the fact that soft cavity radii, instead of the corresponding hard-sphere values, were used in their comparison.

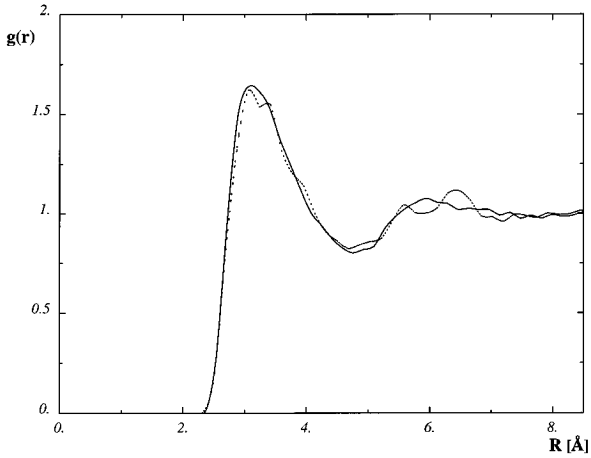

Figure 3. Radial distribution functions $g(r)$ of the water oxygens around cavities computed from a 50 ps (- - -) and a 0.5 ns (—) RP simulation. The radius of the corresponding hard sphere cavity is 1.314 Å.

3. Thermodynamic Considerations. When one leaves the domain of molecular dimensions and deals with a macroscopic cavity, it is possible to express the free energy of cavity formation by means of thermodynamic parameters rather than by a statistical method.[5] Thermodynamic considerations demand the same quadratic polynomial form as does the SP theory (see eq 7). In particular, the comparison between the SP equation and the thermodynamic expression reveals a correspondence between the coefficient of the quadratic term and the surface tension[5] ($=K_2/4\pi$) since this term is related to the work necessary to expand the cavity−solvent interface.

RP and TP predict a surface tension of 56 cal·mol^{-1}·Å^{-2} for hexane, which is more than double the experimental value (26 cal·mol^{-1}·Å^{-2}). For water, the agreement with the experimental surface tension (102 cal·mol^{-1}·Å^{-2}) is better with RP (96 cal·mol^{-1}·Å^{-2}) than with TP (125 cal·mol^{-1}·Å^{-2}). It has been questioned whether it is reasonable to fit a model of a macroscopic form to ΔA_c values for small size cavities[10] and whether the surface tension in the thermodynamic expression for ΔA_c can be approximated by the interfacial tension between a liquid and its vapor.[5,10] Moreover, the surface tension values of the model used for hexane and for water might not reproduce the experimental surface tension for the liquid−vapor interface.

Distribution of the Water Molecules around Cavities in RP and TP. Radial distribution functions $g(r)$ of the water oxygens around the cavities were computed using configurations from the TP and RP simulations. This was done for a range of cavity radii (1.31 ± 0.05 Å) in TP and for a cavity radius of 1.314 Å in RP. Two RP trajectories were used to compute the $g(r)$. One corresponds to the 50 ps production run generated at the corresponding λ value, for the purpose of the free energy calculations. The other, also generated at the same λ value, was 10 times longer (0.5 ns). Figure 3, which displays the $g(r)$ obtained for these two trajectories, shows that the $g(r)$ from the shorter trajectory has its first peak not as well-defined and a more wobbly tail than the $g(r)$ from the longer simulations.

The TP $g(r)$, shown in Figure 4, presents features similar to that previously computed from TIP4P water simulations using the same method.[25] In the latter study, the curve departs at a shorter distance and exhibits a lower first peak, which could result from the use of a smaller water diameter (2.8 versus 3.17 Å).

The RP $g(r)$ computed from the 0.5 ns simulation is compared to that of TP in Figure 4. The TP curve rises abruptly whereas the RP curve slopes upwards more gradually but starts to do so at shorter distances. In the TP curve, the first peak is well

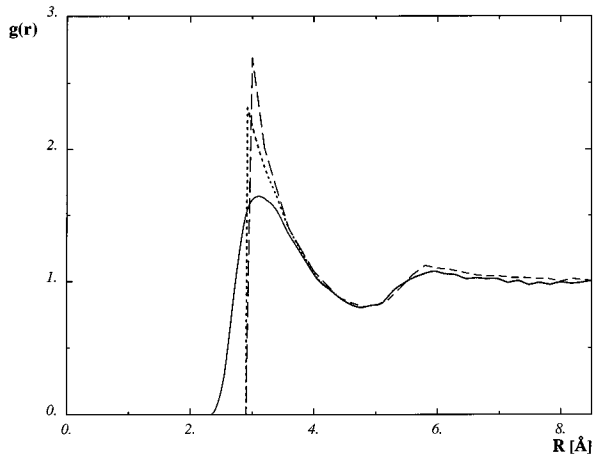

Figure 4. Comparison of the radial distribution functions $g(r)$ computed for the water oxygens around cavities. For TP (− − −), with cavity radii ranging between 1.305 and 1.315 Å. For RP simulations, the $g(r)$ (—) and the corresponding function weighted by $\exp(V_{cav}/RT)$ (- - -) are computed for a hard cavity radius of 1.314 Å.

marked and occurs at 2.9 Å. The RP curve presents a much broader peak centered at about 3.1 Å. These differences can be explained by the soft character of the RP cavity compared to the intrinsic hard character of the spherical cavities in TP.

The RP $g(r)$ weighted by the factor $\exp(V_{cav}/RT)$[19] represents the $g(r)$ for a corresponding hard sphere cavity. This distribution function is shown in Figure 4 for distances larger than 2.9 Å. Interestingly, the first peak of the weighted RP $g(r)$ is lower than that of TP, indicating that the number of solvent molecules in the neighborhood of the cavity is higher in the TP than in the RP simulations. The same conclusion holds for the RP weighted $g(r)$ computed from the 50 ps simulation (data not shown). The higher number of water−cavity contacts is consistent with the ΔA_c value being higher in the TP than in the RP calculations, for the cavity radius considered here (see Figure 2).

Conclusions

Two different computational procedures, the repulsive particle (RP) and the test particle (TP) methods, as well as scale particle theory were used in this study to evaluate the free energy of cavity formation in liquid water and in hexane as a function of the cavity size.

It was found that for sufficiently large cavities, the RP procedure yields higher free energies in water than in hexane, in accord with previous findings based on calculations with the TP method. Considering that the fractional free volume is the same in hexane and water, we conclude, as have authors before us, that in water, the free volume is distributed in smaller packets than in hexane.

We find that the ΔA_c values and their cavity size dependence are different in the RP and TP computations in water. In particular, the free energy for forming molecular size cavities in water is significantly higher with TP than with RP. Why this occurs is not completely clear. The only fundamental difference between the two methods is that RP deals with soft cavities whereas TP considers hard cavities. This was taken into account in the analysis by deriving in the RP calculations the hard sphere radius equivalent to the soft cavity description, using the AWC procedure. It is possible nevertheless that this procedure becomes less reliable when dealing with very soft potentials, in particular for large cavities.[26]

Analysis of the distribution of water molecules around cavities, computed for a cavity radius of ∼1.3 Å, reveals that the water molecules are more tightly packed around the cavity in the TP than in the RP simulations. This would make it easier to insert a particle into the solvent in the RP simulations, in agreement with the lower free energy values computed using this method.

These latter data therefore suggest that the observed discrepancy could stem also from differences in the molecular simulations. Though the trajectories generated in the RP and TP simulations both last 1 ns and more, this may not be enough to reach convergence. Furthermore, the RP simulations were performed with a somewhat smaller box of water molecules (216 molecules) than in the TP simulations (343 molecules). We suggest that performing the simulations under better controlled and identical conditions should bring the two methods to converge to the same result. This could be readily checked by performing longer simulations under constant pressure, using the larger number of water molecules. With regard to the RP simulations, it could be also useful to grow the cavity from different initial conditions or to eliminate an existing cavity by gradually reducing its size to zero.

Acknowledgment. The Belgian program of Interuniversity Poles of Attraction initiated by the Belgian State, Prime Minister's Office for Science, Technology and Culture, is gratefully acknowledged for support. I.T.O. acknowledges support from J.N.I.C.T. (projecto ciência BM/2913/92-RM, Portugal). M.P. is a research associate at the National Fund for Scientific Research (Belgium).

References and Notes

(1) Kauzmann, W. *Adv. Protein Chem.* **1959**, *14*, 1.
(2) Tanford, C. *The Hydrophobic Effect: Formation of Micelles and Biological Membranes*; Wiley Interscience: New York, 1973.
(3) Widom, B. *J. Chem. Phys.* **1982**, *86*, 869.
(4) Lee, B. *Biopolymers* **1991**, *31*, 993.
(5) Reiss, H. *Adv. Chem. Phys.* **1965**, *9*, 1.
(6) Pierotti, R. A. *J. Phys. Chem.* **1965**, *69*, 281.
(7) Pierotti, R. A. *Chem. Rev.* **1976**, *76*, 717.
(8) Stillinger, F. H. *J. Solution Chem.* **1973**, *2*, 141.
(9) Lucas, M. *J. Phys. Chem.* **1976**, *80*, 359.
(10) Pohorille, A.; Pratt, L. R. *J. Am. Chem. Soc.* **1990**, *112*, 5066.
(11) Pohorille, A.; Pratt, L. R. *Proc. Natl. Acad. Sci. U.S.A.* **1992**, *89*, 2995.
(12) Lee, B. *J. Chem. Phys.* **1985**, *83*, 2421.
(13) Madan, B.; Lee, B. *Biophys. Chem.* **1994**, *51*, 279.
(14) Postma, J. P. M.; Berendsen, H. J. C.; Haak, J. R. *Faraday Symp. Chem. Soc.* **1982**, *17*, 55.
(15) Kirkwood, J. G. *J. Chem. Phys.* **1935**, *3*, 300.
(16) Brooks, B. R.; Bruccoleri, R. E.; Olafson, D.; States, D.; Swaminathan, S.; Karplus, M. *J. Comput. Chem.* **1983**, *4*, 187.
(17) Jorgensen, W. L.; Madura, J. D.; Swenson, C. J. *J. Am. Chem. Soc.* **1984**, *106*, 6638.
(18) Berendsen, H. J. C.; Postma, J. P. M.; van Gunsteren, W. F.; Hermans, J. *Intermolecular Forces*; Pullman, B., Ed.; Reidel: Dordrecht, 1981; p 331.
(19) Andersen, H. C.; Weeks, J. D.; Chandler, D. *Phys. Rev. A* **1971**, *4*, 1597.
(20) Verlet, L.; Weiss, J.-J. *Phys. Rev. A* **1972**, *5*, 939.
(21) Hansen, J.-P.; McDonald, J. R. *Theory of Simple Liquids*; Academic Press: London, 1976; p 172.
(22) Ben-Amotz, D.; Herschbach, D. R. *J. Phys. Chem.* **1990**, *94*, 1038.
(23) Simonson, T. *Mol. Phys.* **1993**, *80*, 441.
(24) Swope, W. C.; Andersen, H. C.; Berens, P. H.; Wilson, K. R. *J. Chem. Phys.* **1982**, *76*, 637.
(25) Pratt, L. R.; Pohorille, A. Water-Biomolecule Interactions: *Conference Proceedings of the EBSA;* Palma, M. U., Palma-Vitorelli, M. B., Parak, F., Eds.; EBSA: New York, 1992; p 261.
(26) Pratt, L. R. *Annu. Rev. Phys. Chem.* **1985**, *36*, 433.

JP952906A